Bistable moving optical solitons in resonant photonic crystals

R. A. Vlasov* and A. M. Lemeza†

B.I. Stepanov Institute of Physics of the National Academy of Science of Belarus, 68 Nezavisimosti Ave., Minsk, BY-220072 Belarus

(Received 16 March 2011; published 16 August 2011)

We consider some new aspects of the formation of moving optical solitons in a medium of Bragg-type resonant grating doped with two-level atoms. For generality, account is taken of the local-field effect assisted by a sufficiently high density of resonant atoms. It is established analytically that there exists a family of soliton solutions to the two-wave Maxwell-Bloch system of equations, with these solitons exhibiting bistable properties. The existence of bistable solitons and their properties are confirmed by numerical simulations.

DOI: 10.1103/PhysRevA.84.023828 PACS number(s): 42.65.Tg, 42.70.Qs, 42.25.Bs, 05.45.Yv

I. INTRODUCTION

Nowadays the nonlinear interaction of ultrashort optical pulses with periodic resonant media is of practical significance. This is due to the search for novel properties of pulse propagation which are expected to find applications of considerable promise. Active investigations of pulse propagation through periodic resonantly absorbing media began in the mid 1980s and are actively being continued at present. Mantsyzov was the first to derive the so-called two-wave Maxwell-Bloch system of equations describing the coherent interaction of light with a one-dimensional periodic medium (Bragg grating) represented as a periodical array of thin layers of two-level atoms [1]. Further studies were devoted to the dynamics of pulse propagation in Bragg gratings under different conditions. In particular, they were concerned with the formation of solitons in the case of a weak violation of the Bragg conditions [2], investigations of oscillating solitonlike solutions influenced by inhomogeneous broadening spectra of two-level atoms [2], and the delay of pulse reflection from Bragg gratings [3]. Mention should also be made of the theoretical prediction of forming an optical zumeron [4] and oscillating gap 2π pulses [5] in resonantly absorbing lattices. The results of Mantsyzov's research, as well as extensive literature on the problem of optics of periodic media are reviewed in his monograph [6].

The next important step concerning research into the dynamics of pulses in periodic media was an extension of the system of equations [1] to the case of a spatial modulation of the refractive index of a host medium where the layers of resonant atoms are located. The complete derivation of a system of equations, as well as particular solutions for "zero-velocity" dark and bright solitons, can be found in Refs. [7,8]. In spite of a detailed analysis of zero-velocity solitons, the moving solitonlike analytical solution cannot be found, strictly speaking, from zero-velocity soliton solutions because of the absence of Galilean or Lorentzian invariance of the system (see [7] for details). The one-parameter subfamily of solitons is found in [9] where the solution is expressed in a sech-like form at the band-gap edge. An alternative method for finding an analytical solitonlike solution is to asymptotically reduce the system of equations to nonlinear Schrödinger equation [7]. When simulated numerically, the stable moving solitons were obtained by adding the phase modulation to the zero-velocity solitons [10].

In Ref. [11], attention was paid to the fact that in periodic resonant structures the formation of stationary pulses can markedly be affected by the dipole-dipole interactions (local field) [12]. The dipole-dipole interaction is known to result in a number of new phenomena: Lorentz shift [13], ultrafast optical switching [14], enhancement of inversionless gain and refractive index without absorption [15], reduction of the electromagnetically induced transparency [16], enhancement of the spontaneous emission rate in a dielectric [17], modification of the superradiant amplification [18], and incoherent solitons and phase modulation of self-induced transparency solitons [19,20].

As shown in Ref. [11], the influence of the local field substantially changes the conditions of existence of zero-velocity solitons. This is shown analytically and numerically. However, the study of moving solitons is restricted to the numerical simulation similar to that conducted in Ref. [10], where the moving pulse is obtained from the zero-velocity soliton by introducing an artificial phase modulation.

Based on numerical simulations, the effect of the local field on the formation of ultrashort pulses in a medium with the modulated refractive index (for a homogeneous distribution of the resonant level particles along the sample) is considered in Refs. [21,22]. It is shown that the local field leads to a phase change, whereas the amplitude changes due to the influence of dipole-dipole interactions are rather small.

It is pertinent to emphasize that the majority of the above-mentioned studies concerning moving solitons are predominantly simulated numerically. Analytical results are appropriate to simplified models or specific cases. That is, a sufficiently general analytical approach is lacking in the current theory. It is self-evident that some theoretical aspects of the problem under study are not yet fully understood.

The present paper deals with the self-induced transparency (SIT) in resonant photonic crystals where the interplay of the resonant nonlinearity, Bragg reflection, and near dipole-dipole interaction (local field) takes place. It is our intention here to reveal the existence and explain the properties of SIT solitons. Their formation is examined analytically and numerically. Particular emphasis is placed on the analytical solution, because it is just what we are going to benefit from to arrive at the bistability. As applied to temporal solitons, by the bistability is meant the existence of solitons in two steady states (in one or another), their envelopes in these states differing,

*r.vlasov@dragon.bas-net.by
†azemel@gmail.com

for example, in amplitude (peak) at the same duration [23,24]. Of course, the concept of two steady states must be common for bistable temporal solitons of any nature.

The bistability seems by itself to be interesting as a novel property of SIT solitons in periodic media. In addition, the matter may also concern potential applications associated with their controllable propagation.

The rest of our paper is structured as follows. In the second section we address the model of propagation of an electromagnetic wave through a resonantly absorbing medium with a one-dimensional modulation of the refractive index. The third section is devoted to finding solitonlike analytical solutions of the equations used in our model, with their properties being discussed. In the fourth section we numerically check the stability of the soliton solutions obtained, and consider their interaction and formation. At that, the fourth-order Runge-Kutta method used in our numerical experiments is treated in detail. At the end of paper we will discuss the possibility of the experimental realization of the found regimes of propagating and perform the estimation of the parameters of the problem. In conclusion, in the sixth section, the basic results are briefly discussed.

II. BASIC EQUATIONS

We consider a medium with the one-dimensional periodic modulation of the refractive index $n(z)$ along the direction of propagation of an electromagnetic wave. It is assumed that the one-dimensional periodic grating has a period d and resonant centers are located in the maxima of the refractive index $z = z_j$. The length of these layers is much smaller than the period of the periodic grating. At the same time, we assume that the "local" density $\sigma(z_j)$ of two-level atoms is great enough so that the dipole-dipole interactions cannot be neglected.

To be more consequent in our presentation, let us recall some important steps of deriving model equations, which are covered in detail in Refs. [7,8] without allowance for the local field. The local-field correction to the system of [7,8] was introduced for the first time in [11], to our knowledge. Here we present the main steps of deriving a system of equations describing the propagation of light in periodic resonant media (this system is often called a two-wave Maxwell-Bloch system). While deriving it, we follow Refs. [7,8,11].

A. Subsystem of the Bloch equations

To derive the Bloch equations for two-level atoms, we start from the Heisenberg equation of motion for operators,

$$i\hbar\frac{d\hat{A}}{dt} = [\hat{A},\hat{H}], \tag{1}$$

and the Hamiltonian of a two-level atom in the electromagnetic field,

$$\hat{H} = \frac{\hbar\omega_0}{2}\hat{w} - \mathcal{E}\hat{d}, \tag{2}$$

where $\hat{w} = |e\rangle\langle e| - |g\rangle\langle g|$ is the atomic inversion operator, $|e\rangle$ and $|g\rangle$ are the excited and ground states, respectively, ω_0 is the resonant transition frequency of the two-level atom, $\mathcal{E}$ is the magnitude of the electromagnetic field vector $\mathbf{E}$, $\hat{d}$ is the projection of the atomic dipole moment operator $\hat{\mathbf{d}}$ to the vector of electromagnetic field $\mathbf{E}$, and $\hbar$ is Planck's constant.

The dipole momentum operator can be introduced in the form

$$\hat{d} = \frac{\mu}{2}(\hat{P} + \hat{P}^{\dagger}), \tag{3}$$

where μ is the dipole matrix element (is to be real) and the two-level atom polarization operator can be written as

$$\hat{P} = 2|g\rangle\langle e|. \tag{4}$$

In what follows we define the polarization and population inversion as $p = ie^{i\omega_c t}\langle\hat{P}\rangle$ and $w = \langle\hat{w}\rangle$; the macroscopic field $\mathcal{E}$ is represented as

$$\mathcal{E}(z,t) = E(z,t)e^{-i\omega_c t} + \text{c.c.}, \tag{5}$$

where ω_c is the central frequency of the fundamental gap (this will be clarified below), and c.c. denotes the complex conjugation.

Using the Heisenberg equation of motion, we obtain the Bloch equations of evolution of the two-level atom in the electromagnetic field in the rotating wave approximation:

$$\frac{\partial p}{\partial t} = -i(\omega_0 - \omega_c)p + \frac{2\mu}{\hbar}wE, \tag{6}$$

$$\frac{\partial w}{\partial t} = -\frac{\mu}{\hbar}(p^*E + pE^*). \tag{7}$$

To take into account the influence of the local field, the macroscopic field in Eqs. (6) and (7) should be corrected for the local field. According to Ref. [18], the local field $\mathcal{E}_{\text{loc}}$ can be expressed as

$$\mathcal{E}_{\text{loc}} = \mathcal{E} + \tfrac{1}{3}\mathcal{P}_l + \tfrac{1}{3}\mathcal{P}_{nl}, \tag{8}$$

where $\mathcal{P}_l = 3\frac{n^2-1}{n^2+2}\mathcal{E}_{\text{loc}}$ is the linear polarization of dielectric media with the refractive index n and $\mathcal{P}_{\text{nl}}$ is the nonlinear polarization of the two-level atoms.

Expressing the local field $\mathcal{E}_{\text{loc}}$ in terms of macroscopic field $\mathcal{E}$ and nonlinear polarization $\mathcal{P}_{\text{nl}}$, we obtain

$$\mathcal{E}_{\text{loc}} = \frac{n^2+2}{3}\left(\mathcal{E} + \frac{1}{3}\mathcal{P}_{\text{nl}}\right). \tag{9}$$

The nonlinear polarization $\mathcal{P}_{\text{nl}}$ can be expressed as

$$\begin{aligned}\mathcal{P}_{\text{nl}}(z,t) &= 4\pi\sigma(z)\langle\hat{d}\rangle \\ &= -2\pi i\sigma(z)\mu p e^{-i\omega_c t} + \text{c.c.},\end{aligned} \tag{10}$$

where $\sigma(z)$ is the density of two-level atoms.

In view of this and replacing the macroscopic field in Eqs. (6) and (7) by the local one ($\mathcal{E} \to \mathcal{E}_{\text{loc}}$), the Bloch equations then become

$$\frac{\partial p}{\partial t} = -i(\omega_0 - \omega_c + \omega_L w)p + \frac{2\mu}{\hbar}\frac{n^2+2}{3}wE, \tag{11}$$

$$\frac{\partial w}{\partial t} = -\frac{\mu}{\hbar}\frac{n^2+2}{3}(p^*E + pE^*), \tag{12}$$

where

$$\omega_L = \frac{4\pi\mu^2\sigma}{\hbar}\frac{n^2+2}{9}$$

is the Lorentz frequency.

One can see from this system that the local-field effect results in a nonlinearity determined by the interplay between w and p.

B. Subsystem of Maxwell equations

The propagaton of light through the periodic media is governed by the one-dimensional Maxwell equation

$$\left(c^2\frac{\partial^2}{\partial z^2}-n(z)^2\frac{\partial^2}{\partial t^2}\right)\mathcal{E}(z,t)=\frac{\partial^2}{\partial t^2}\mathcal{P}_{\rm nl}(z,t), \tag{13}$$

where $n(z)$ is the refractive index and c is the velocity of light in vacuum. Because of the periodic modulation of refractive index along the media, the square of $n(z)$ can be expressed as Fourier series

$$n(z)^2=n_0^2\left(1+\sum_{j=1}^{\infty}a_j\,\cos(2jk_cz)\right), \tag{14}$$

where $k_c=\pi/d$ (and $\omega_c=k_cc/n_0$).

On the other hand, the electromagnetic field can be represented in the form

$$\mathcal{E}(z,t)=[E_F(z,t)e^{ik_cz}+E_B(z,t)e^{-ik_cz}]e^{-i\omega_ct}+\text{c.c.} \tag{15}$$

In other words, the original envelope of the electromagnetic field $E(z,t)$ in Eq. (5) is split into the forward $E_F(z,t)$ and backward $E_B(z,t)$ propagating components. Then, substituting Eqs. (14) and (15) into Eq. (13) and performing slowly varying envelopes approximation

$$\left|\frac{\partial^2E_{F,B}(z,t)}{\partial z^2}\right|\ll\left|k_c\frac{\partial E_{F,B}(z,t)}{\partial z}\right|, \tag{16}$$

$$\left|\frac{\partial^2E_{F,B}(z,t)}{\partial t^2}\right|\ll\left|\omega_c\frac{\partial E_{F,B}(z,t)}{\partial t}\right|, \tag{17}$$

after averaging over the wavelength $\lambda=2\pi/k_c$ and period $T=2\pi/\omega_c$, we obtain the set of equations describing the evolution of the forward and backward field components,

$$\frac{\partial E_F}{\partial t}+\frac{c}{n_0}\frac{\partial E_F}{\partial z}-\frac{ia_1\omega_c}{4}E_B=\frac{i}{2n_0^2\omega_c}P_-, \tag{18}$$

$$\frac{\partial E_B}{\partial t}-\frac{c}{n_0}\frac{\partial E_B}{\partial z}-\frac{ia_1\omega_c}{4}E_F=\frac{i}{2n_0^2\omega_c}P_+, \tag{19}$$

where, by definition,

$$P_\pm=\left\langle\frac{\partial^2\mathcal{P}_{\rm nl}}{\partial t^2}e^{\pm ik_cz+i\omega_ct}\right\rangle_{\lambda,T}.$$

In Eqs. (18) and (19), averaging over λ and T is denoted as $\langle X(z,t)\rangle_{\lambda,T}=\frac{1}{\lambda T}\int_\lambda\int_T X(z,t)dt\,dz$.

As discussed earlier, thin (much shorter than $1/k_c$) layers of two-level atoms are located in maxima of the periodically modulated refractive index, and the density of atoms is high enough so that the local field can be significant. While averaging the right-hand sides of Eqs. (18) and (19), we assume that the distribution of two-level atoms can be approximated by the function

$$\sigma(z)=\frac{\sigma_0\lambda}{2}\sum_j\delta(z-z_j), \tag{20}$$

where the Dirac delta function $\delta(z-z_j)$ indicates that atoms are placed in the maxima of the refractive index $z_j=j\lambda/2$ and σ_0 is the density averaged over wavelength. Substituting Eq. (20) into Eqs. (18) and (19), applying slowly varying amplitude approximation in time for polarization $\mathcal{P}_{\rm nl}$ and averaging over the period and wavelength, we get the following equations:

$$\begin{aligned}P_\pm&=\left\langle\frac{\partial^2\mathcal{P}_{\rm nl}}{\partial t^2}e^{\pm ik_cz+i\omega_ct}\right\rangle_{\lambda,T}\\&=\left\langle-2\pi i\mu\sigma(z)e^{\pm ik_cz+i\omega_ct}\frac{\partial^2}{\partial t^2}(pe^{-i\omega_ct}-p^*e^{i\omega_ct})\right\rangle_{\lambda,T}\\&\approx-2\pi i\mu\omega_c^2\langle\sigma(z)pe^{\pm ik_cz}\rangle_\lambda\\&=-2\pi i\mu\omega_c^2\frac{1}{\lambda}\int_{z-\lambda/2}^{z+\lambda/2}\frac{\sigma_0\lambda}{2}\sum_j\delta(\xi-\xi_j)p(\xi)e^{\pm ik_c\xi}\,d\xi\\&=-2\pi i\mu\omega_c^2\sigma_0p.\end{aligned} \tag{21}$$

C. Dimensionless form of the equations

Now we are in a position to write the complete set of relevant two-wave Maxwell-Bloch equations which read

$$\frac{\partial E_F}{\partial t}+\frac{c}{n_0}\frac{\partial E_F}{\partial z}-\frac{ia_1\omega_c}{4}E_B=\frac{\pi\mu\omega_c\sigma_0}{n_0^2}p, \tag{22}$$

$$\frac{\partial E_B}{\partial t}-\frac{c}{n_0}\frac{\partial E_B}{\partial z}-\frac{ia_1\omega_c}{4}E_F=\frac{\pi\mu\omega_c\sigma_0}{n_0^2}p, \tag{23}$$

$$\frac{\partial p}{\partial t}=-i(\omega_0-\omega_c+\omega_Lw)p+\frac{2\mu}{\hbar}\frac{n(z_j)^2+2}{3}w(E_F+E_B), \tag{24}$$

$$\frac{\partial w}{\partial t}=-\frac{\mu}{\hbar}\frac{n(z_j)^2+2}{3}[p^*(E_F+E_B)+\text{c.c.}], \tag{25}$$

where $n(z_j)$ indicates that the refractive index is calculated in the points where the thin layers of two-level atoms are located (namely, in maxima). For the further analysis it is convenient to introduce the dimensionless variables and parameters in accordance with the following normalization:

$$\Omega_{F,B}=\frac{2\mu\tau_0}{\hbar}\frac{n(z_j)^2+2}{3}E_{F,B},\quad\tau=\frac{t}{\tau_0},\quad\zeta=\frac{n_0}{\tau_0c}z,$$

$$\delta=(\omega_0-\omega_c)\tau_0,\quad\varepsilon=\omega_L\tau_0=\frac{4\pi\mu^2\sigma}{\hbar}\frac{n(z_j)^2+2}{9}\tau_0,$$

$$\eta=\frac{a_1\omega_c\tau_0}{4},\quad\tau_0^2=\frac{3n_0^2\hbar}{2\pi\mu^2\omega_c\sigma_0[n(z_j)^2+2]}.$$

Here τ and ζ are the dimensionless time and space coordinate, δ is the dimensionless detuning of resonant frequency of two-level atoms ω_0 from the central frequency of the fundamental gap ω_c, ε is the local field parameter, η is the ratio of characteristic absorption distance to the Bragg reflection distance, and τ_0 is the characteristic absorption time. Thereafter the complete system (22)–(25) can be written in the form

$$\frac{\partial\Omega_F}{\partial\tau}+\frac{\partial\Omega_F}{\partial\zeta}=i\eta\Omega_B+p, \tag{26}$$

$$\frac{\partial \Omega_B}{\partial \tau} - \frac{\partial \Omega_B}{\partial \zeta} = i\eta\Omega_F + p, \tag{27}$$

$$\frac{\partial p}{\partial \tau} = -i(\delta + \varepsilon w)p + w(\Omega_F + \Omega_B), \tag{28}$$

$$\frac{\partial w}{\partial \tau} = -\frac{1}{2}[p^*(\Omega_F + \Omega_B) + p(\Omega_F + \Omega_B)^*]. \tag{29}$$

Equations (26)–(29) may, however, be rearranged to read as in Refs. [7–11]. This is brought about by introducing the new variables $\Sigma_\pm = \Omega_F \pm \Omega_B$ and recasting the equations of the Maxwell subsystem of equations into the second-order partial differential equations

$$\left(\frac{\partial^2}{\partial \tau^2} - \frac{\partial^2}{\partial \zeta^2}\right)\Sigma_+ = 2\frac{\partial}{\partial \tau}p + 2i\eta p - \eta^2\Sigma_+, \tag{30}$$

$$\left(\frac{\partial^2}{\partial \tau^2} - \frac{\partial^2}{\partial \zeta^2}\right)\Sigma_- = -2\frac{\partial}{\partial \zeta}p - \eta^2\Sigma_-, \tag{31}$$

$$\frac{\partial p}{\partial \tau} = -i(\delta + \varepsilon w)p + w\Sigma_+, \tag{32}$$

$$\frac{\partial w}{\partial \tau} = -\frac{1}{2}(p^*\Sigma_+ + p\Sigma_+^*). \tag{33}$$

In this work use is made of system (26)–(29), which is more convenient for analytical calculations and numerical simulations. That is, for our purposes the system in question is more useful as it stands.

III. ANALYTICAL SOLUTION

We seek a solitonlike solution of system (26)–(29) in the form

$$\begin{aligned} \Omega_F(\tau,\zeta) &= F(u)\exp(-i\eta\tau), \\ \Omega_B(\tau,\zeta) &= B(u)\exp(-i\eta\tau), \\ p(\tau,\zeta) &= Q(u)\exp(-i\eta\tau), \\ w(\tau,\zeta) &= W(u)\exp(-i\eta\tau), \end{aligned} \tag{34}$$

where $u = \tau - \zeta/v$. In so doing, unlike [9], a shift of the carrying frequency of the soliton toward the band-gap edge is taken into account from the very outset, but the field envelope is not yet specified and is to be determined. Substituting Eq. (34) into system (26)–(29), we get the following set of equations:

$$\left(\frac{v-1}{v}\right)\frac{\partial F}{\partial u} = Q + i\eta(F + B), \tag{35}$$

$$\left(\frac{v+1}{v}\right)\frac{\partial B}{\partial u} = Q + i\eta(F + B), \tag{36}$$

$$\frac{\partial Q}{\partial \tau} = W(F + B) - i(\delta - \eta + \varepsilon W)Q, \tag{37}$$

$$\frac{\partial W}{\partial u} = -\frac{1}{2}[Q^*(F + B) + Q(F + B)^*]. \tag{38}$$

From Eqs. (35) and (36) it is easy to find the relation between $F(u)$ and $B(u)$:

$$B = C_1 + \frac{v-1}{v+1}F, \tag{39}$$

where C_1 is a constant of integration. We are interested only in bright solitons, and for this reason C_1 should be set to zero to meet the conditions at infinity $[F(\pm\infty) = B(\pm\infty) = 0]$. Then introducing a new function

$$\Phi = F + B = F + \frac{v-1}{v+1}F = \frac{2v}{v+1}F, \tag{40}$$

one can obtain the system

$$\left(\frac{v^2-1}{2v^2}\right)\frac{\partial \Phi}{\partial u} = Q + i\eta\Phi, \tag{41}$$

$$\frac{\partial Q}{\partial u} = W\Phi - i(\delta - \eta + \varepsilon W)Q, \tag{42}$$

$$\frac{\partial W}{\partial u} = -\frac{1}{2}(Q^*\Phi + Q\Phi^*). \tag{43}$$

This set of equations is quite similar to the Maxwell-Bloch system of equations for optically dense resonant media used in Refs. [19,20], where the dipole-dipole interactions of the two-level atoms are taken into account. As is shown in Refs. [19,20], such an extended Maxwell-Bloch system of equations has a family of solitons with a nonlinear phase modulation. Below, seeking a soliton solution, we will follow the approach used in Refs. [19,20]. Thereupon Eq. (41) can be solved for Q and the solution may be substituted into other equations. These manipulations give

$$\begin{aligned} \gamma\frac{\partial^2\Phi}{\partial u^2} + i\left[\gamma(\delta - \eta + \varepsilon W) - \eta\right]\frac{\partial \Phi}{\partial u} \\ +[(\delta - \eta)\eta + (\varepsilon\eta - 1)W]\Phi = 0, \end{aligned} \tag{44}$$

$$\frac{\partial W}{\partial u} = -\gamma\left(\frac{\partial \Phi^*}{\partial u}\Phi + \frac{\partial \Phi}{\partial u}\Phi^*\right), \tag{45}$$

where $\gamma = (\frac{v^2-1}{4v^2})$.

The solution of Eq. (45) is then

$$W = -1 - \gamma\Phi^*\Phi, \tag{46}$$

where the conditions at infinity correspond to the absence of electromagnetic field $[\Phi(\pm\infty) = 0]$ and population inversion of two-level atoms $[W(\pm\infty) = -1]$.

As a result, we arrive at the final equation

$$\begin{aligned} \frac{\partial^2\Phi}{\partial u^2} + i\left[\delta - \eta - \varepsilon\left(1 + \frac{\gamma}{2}|\Phi|^2\right) - \frac{\eta}{\gamma}\right]\frac{\partial \Phi}{\partial u} \\ + \frac{1}{\gamma}\left[(\delta - \eta)\eta + (1 - \varepsilon\eta)\left(1 + \frac{\gamma}{2}|\Phi|^2\right)\right]\Phi = 0. \end{aligned} \tag{47}$$

Equation (47) can be reduced to a set of familiar equations. To this end, let us seek a solution in the form of $\Phi(u) = A(u)\exp[i\psi(u)]$, where $A(u)$ and $\psi(u)$ are real functions. Substituting the $\Phi(u)$ into Eq. (47), one can obtain the two real equations

$$\begin{aligned} \frac{\partial^2 A}{\partial u^2} + \left\{\frac{1}{\gamma} + \frac{\eta}{\gamma}(\delta - \varepsilon - \eta) + \frac{\partial \psi}{\partial u}\left[-\delta + \eta\left(1 + \frac{1}{\gamma}\right) - \frac{\partial \psi}{\partial u}\right]\right\}A \\ + \frac{1}{2}\left[1 - \varepsilon\left(\eta - \gamma\frac{\partial \psi}{\partial u}\right)\right]A^3 = 0, \end{aligned} \tag{48}$$

$$A\frac{\partial^2\psi}{\partial u^2} + 2\frac{\partial \psi}{\partial u}\frac{\partial A}{\partial u} - \frac{\partial A}{\partial u}\left[\frac{\gamma}{2}A^2 - \delta + \varepsilon + \eta\left(1 + \frac{1}{\gamma}\right)\right] = 0. \tag{49}$$

By multiplying Eq. (49) by $A(u)$ and subjecting it to the condition $A(\pm\infty) = 0$, integration can be easily performed to

yield

$$\frac{\partial\psi}{\partial u} = \frac{4\left[\eta + \gamma(\varepsilon - \delta + \eta)\right] + \gamma^2\varepsilon A^2}{8\gamma}. \tag{50}$$

By substituting Eq. (50) into Eq. (48) and integrating it at the condition $A(\pm\infty) = 0$, the final equation for the amplitude is obtained to read

$$\left(\frac{\partial A}{\partial u}\right)^2 = a_2A^2 - a_4A^4 - a_6A^6, \tag{51}$$

where the coefficients are

$$a_2 = -\frac{\eta^2 + \gamma^2(\delta - \varepsilon - \eta)^2 + 2\gamma\left[2 + \eta(\delta - \varepsilon - \eta)\right]}{4\gamma^2},$$

$$a_4 = \frac{1}{8}\left\{2 - \varepsilon\left[\eta + \gamma(\delta - \varepsilon - \eta)\right]\right\}, \quad a_6 = \frac{\gamma^2\varepsilon^2}{64}.$$

The soliton solution of Eq. (51) is

$$A(u) = \sqrt{\frac{2a_2}{a_4 + \sqrt{a_4^2 + 4a_2a_6}\,\cosh(2u\sqrt{a_2})}}, \tag{52}$$

The phase is found to be

$$\psi(u) = \frac{\left[\eta + \gamma(\varepsilon - \delta + \eta)\right]}{2\gamma}u + \arctan\left(\frac{\left(-a_4 + \sqrt{a_4^2 + 4a_2a_6}\right)}{2\sqrt{a_6a_2}}\tanh(u\sqrt{a_2})\right), \tag{53}$$

where the constant of integration related to a constant phase shift is omitted.

As seen from Eq. (53), the phase modulation is a nonlinear function of the variable u. The nonlinear part of the phase modulation [as is seen from Eq. (50)] is a consequence of the dipole-dipole interaction of two-level atoms; it disappears when the local field is negligibly small.

From Eq. (52), the soliton duration can be defined as

$$\tau_p = \frac{1}{\sqrt{a_2}}. \tag{54}$$

By combining Eq. (54) and the previously defined expression of γ and a_2, the relationship between the inverse square velocity and pulse duration can be expressed as

$$\frac{1}{v_\pm^2} = \frac{4 + [8 + (\delta - \varepsilon + \eta)^2]\tau_p^2}{4 + [4 + (\delta - \varepsilon)^2 - \eta^2]\tau_p^2 \pm 4\sqrt{-\eta^2\tau_p^2 + [1 + \eta(\delta - \varepsilon - \eta)]\tau_p^4}}, \tag{55}$$

Hence it is immediately evident that the inverse square velocity is a two-valued function of the duration τ_p. This two-valuedness may be regarded as the bistability, and such a property implies that, in general, two envelopes (or states) are allowed for the soliton to exist in either state at the same pulse duration.

At first, let us consider the limiting case where all the parameters tend to zero ($\delta, \varepsilon, \eta \to 0$). There are two asymptotes to Eq. (55): $\frac{1}{v_+^2} \to 1$ and $\frac{1}{v_-^2} \to 1 + \tau_p^2$. The last is derived for the periodic thin layers of two-level atoms in [1], the envelope being of the sech-like form. Obviously, the first limit $\frac{1}{v_+^2} \to 1$ corresponds to the linear pulse propagation without the interaction with resonant atoms. Such a pulse may not be classified among solitons.

The mechanisms underlaying the bistability are determined by the appropriate parameters entering into expression (55). The basic mechanisms are related to the local field (ε) and spatial modulation of the refractive index (η). In the general case the parameters $\delta, \varepsilon, \eta \neq 0$ and the joint action of these mechanisms takes place. Then there is a range of parameters where the function $1/v^2\left(\tau_p\right)$ is bistable and the bistability is most pronounced. Figure 1 demonstrates the branches of Eq. (55) at the parameters $\varepsilon = 0.8$, $\delta = -0.6$, and $\eta = 0.5$. The envelopes of population inversion W and electromagnetic field A [see Eqs. (52) and (46)] of both solitons at $\tau_p = 2.5$ are shown in Fig. 2. The dot-dashed curves correspond to the lower branch of the functions shown in Fig. 1, and the solid curve corresponds to the upper one. While the distinction of the electromagnetic field envelopes is slight, nevertheless it is quite observable. According to Fig. 2, the population inversions differ more significantly, and here it should be noted that the upper branch soliton interacts with two-level atoms more effectively than the lower branch soliton. In addition, the bistability of solitons is most pronounced at short durations. The main reason for this is also a more effective interaction

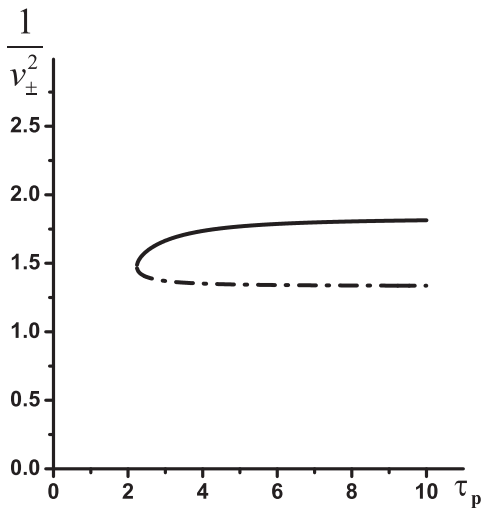

FIG. 1. Inverse square velocity of the soliton versus its duration at $\varepsilon = 0.8$, $\delta = -0.6$, $\eta = 0.5$. The solid line indicates the v_- solution, the dot-dashed line indicates the v_+ solution.

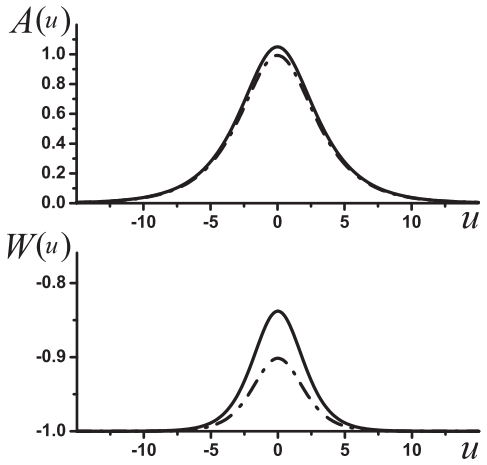

FIG. 2. Envelopes $A(u)$ and $W(u)$ of the bistable solitons as functions of the autowave variable u at $\varepsilon = 0.8$, $\delta = -0.6$, $\eta = 0.5$, and $\tau_p = 2.5$. The solid line indicates the envelopes for the upper branch; the dot-dashed line indicates the soliton of the lower branch of Fig. 1.

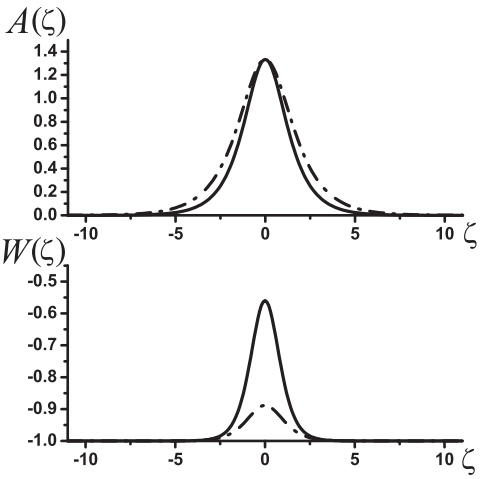

FIG. 4. Envelopes $A(\zeta)$ and $W(\zeta)$ of the bistable solitons as functions of space variable ζ at $\varepsilon = 0.0$, $\delta = -1.0$, $\eta = 0.5$, and $\tau_p = 1.5$. The solid line displays the envelopes for the upper branch; the dot-dashed line displays the soliton of the lower branch of Fig. 3.

of the solitons of both branches of Eq. (55) with resonant atoms.

At the same time it is not unreasonable to single out one mechanism for the purpose of gaining a better insight into its nature. In this connection, an intriguing question arises as to whether there is bistability in the absence of the local field.

At $\varepsilon \to 0$ the pulse envelope approaches a sech-like form and the phase modulation becomes linear. Here the bistability also takes place. Figure 3 illustrates the inverse square velocity versus the pulse duration at $\varepsilon = 0.0$, $\delta = -1.0$, and $\eta = 0.5$. The bistability, as before, is observed in a region of shorter pulse durations ($\tau_p \sim 2$), but it is somewhat modified. This modification permits the amplitudes (maxima) be equal, however, envelopes are distinguished by their extensions along the propagation coordinate ζ. At that the population inversions differ significantly. To clarify the distinction of the bistable solitons more pictorially, in Fig. 4 are exhibited the field envelope $A(\zeta)$ and population inversion $W(\zeta)$ as functions of the space coordinate ζ (the pulse duration is $\tau_p = 1.5$). As seen from Fig. 4, the soliton corresponding to the upper branch is shorter in space than the soliton corresponding to the lower branch, and its interaction with two-level atoms is more effective. Moreover, as follows from Eqs. (39) and (40), the pulses possess the different relations of the forward and backward components of the electromagnetic field due to the velocity distinction. Surprisingly enough, when the spatial modulation is eliminated ($\eta = 0$) and there occurs the local field only ($\varepsilon \neq 0$), the bistability is absent ($v_+ \equiv 1$).

Thus, there is good reason to believe that the modulation of the refractive index is basically responsible for the soliton bistability. However, the influence of the local field enhances the bistable properties. And, as a consequence, there arises the distinction between the field amplitudes, too. Also, when the local field is taken into account, the phase modulation becomes nonlinear.

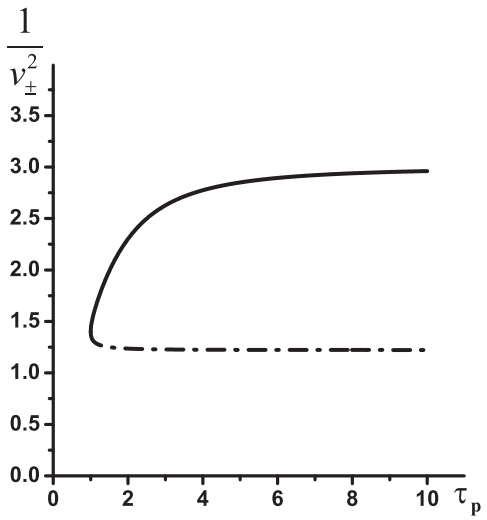

FIG. 3. Inverse square velocity of the soliton versus its duration at $\varepsilon = 0.0$, $\delta = -1.0$, and $\eta = 0.5$.

IV. NUMERICAL SIMULATION

This section is devoted to the numerical investigation of the properties of bistable solitons. We will focus on the stability, formation, and collision of solitons. Our numerical tests are performed with the help of a fourth-order numerical integration scheme which is briefly explained below.

A. Numerical algorithm

For the numerical simulations, we use a modification of the fourth-order method of characteristics developed in Ref. [25] for a system of two nonlinear hyperbolic equations. According to Ref. [25], each equation of system (26)–(29) along the characteristics can be formally written as

$$\frac{\partial y}{\partial x} = f(x,y), \tag{56}$$

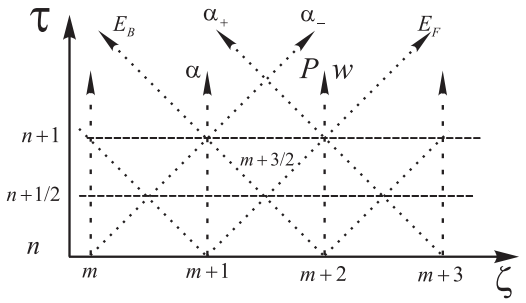

FIG. 5. Integration algorithm scheme. The dotted lines depict the characteristic curves α and $\alpha_{\pm}$. The time and space states are numbered by $n + j/2$ and $m + l/2$, respectively.

and its formal integration can be performed with the help of the following two-step procedure:

$$y_{n+1/2} = y_n + h\{a_{21} f(x_n, y_n) + a_{22} f(x_{n+1/2}, y_{n+1/2}) + a_{23} f\,(x_{n+1}, y_{n+1})\}, \quad (57)$$

$$y_{n+1} = y_n + h\{a_{31} f(x_n, y_n) + a_{32} f(x_{n+1/2}, y_{n+1/2}) + a_{33} f\,(x_{n+1}, y_{n+1})\}, \quad (58)$$

where the coefficients are $a_{21} = 5/24$, $a_{22} = 1/3$, $a_{23} = -1/24$, $a_{31} = 1/6$, $a_{32} = 2/3$, and $a_{33} = 1/6$.

In contrast to the system considered in Ref. [25], system (26)–(29) involves two linear equations (26)and (27) with the characteristics $\alpha_{\pm} = \zeta \pm \tau$ and two nonlinear equations (28) and (29) with the characteristic $\alpha = \tau$. This fact can be taken into account by an appropriate choice of characteristic intersection points and interpolation of data. Our modification of method proposed in Ref. [25] is schematically represented in Fig. 5, where the dotted lines with arrows indicate the characteristics of Eqs. (26)–(29) and the dashed lines show the time layers.

As illustrated in Fig. 5, all the characteristics intersect at points where $\tau = nh$ and $\zeta = mh$. However, to integrate Eqs. (26) and (27) along the characteristics, it is necessary to know a value of polarization at $\tau = (n + 1/2)\,h$ and $\zeta = (m + 3/2)\,h$. These values can be calculated by interpolating data from points where the polarization is known, namely, $\tau = (n + 1/2)\,h$ and $\zeta_l = (m + l)\,h$, where $l = 0,1,2,3$. This is achieved by the fourth-order accurate interpolation algorithm. Accordingly, to integrate Eqs. (28) and (29) along the characteristic, it is also necessary to perform the interpolation of the field components Ω_F and Ω_B to points $\tau = nh$ and $\zeta = mh$.

B. Bistability of solitons

As indicated above, the moving soliton in resonantly absorbing photonic crystals possesses the bistable properties. However, the bistability of a stationary solution does not need to mean the stability of solitons corresponding to the two branches. In order to check the stability of obtained solutions, advantage is taken of the numerical simulations to prove the stability of the solitons (52) and (53). In our simulation, use is made of the analytical solutions of the field components Ω_F and Ω_B, polarization P, and population inversion W, obtained in the previous section, as initial conditions, and then the system is numerically integrated using algorithm (56)–(58).

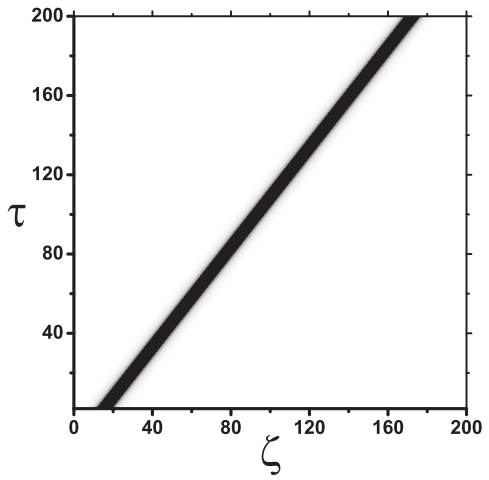

FIG. 6. Evolution of A of the upper branch soliton shown in Fig. 1 at $\tau_p = 2.5$.

Figure 6 shows the evolution of soliton (52)–(53) corresponding to the upper branch of Fig. 1 at $\tau_p = 2.5$. The soliton propagates through the sample without changes at the velocity predicted by analytical expression (55). Soliton (52)–(53) corresponding to the lower branch of Fig. 1 at $\tau_p = 2.5$ demonstrates a similar stable evolution at a higher velocity (see Fig. 7).

So, as seen from Figs. 6 and 7, the bistability of solitons takes place. Here we should also note that solitons corresponding to both branches are formed if the initial conditions of Ω_F, Ω_B, P, and w are taken sufficiently close to the analytically predicted ones. After the transient process, the solitons are formed but their parameters can be slightly different due to changes during the transient process.

C. Stability against perturbations

Figure 8 gives the soliton evolution analogous to that shown on Fig. 6 but in the presence of random noise. The stochastic perturbations are added to all dynamic variables (Ω_F,Ω_B,P,w) and comprise about 10% of amplitude of any variable. As is

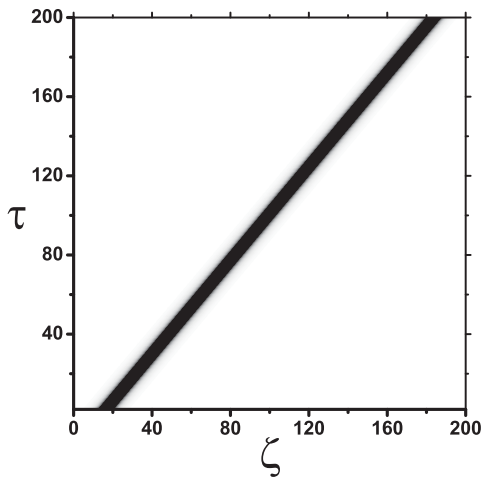

FIG. 7. Evolution of A of the lower branch soliton shown in Fig. 1 at $\tau_p = 2.5$.

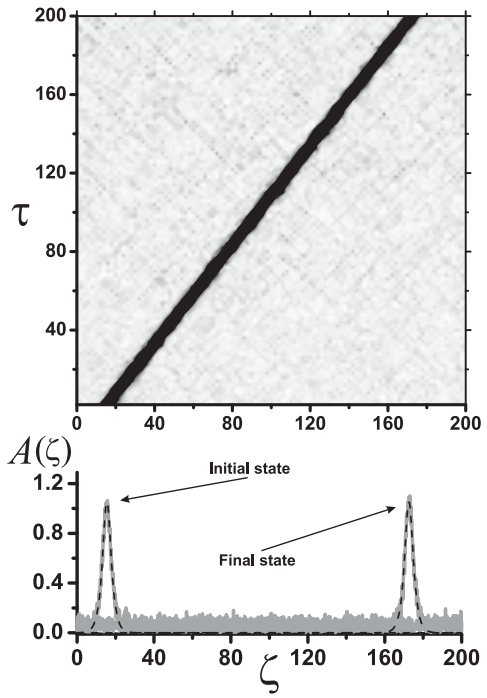

FIG. 8. Evolution of A of the upper branch soliton shown in Fig. 1 at $\tau_p = 2.5$ in the presence of random noise. Initial and final states of evolution are shown below in comparison with corresponding evolution without random noise shown in Fig. 6. The evolutions with noise are denoted by the gray lines, whereas the evolutions without noise are denoted by the dashed black lines.

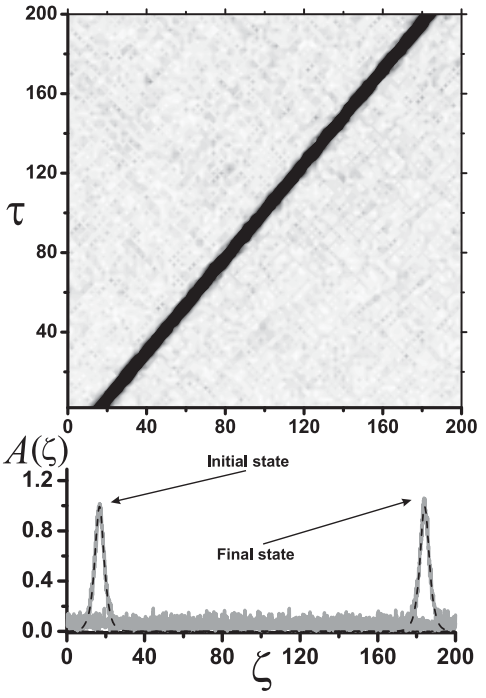

FIG. 9. Evolution of A of the lower branch soliton shown in Fig. 1 at $\tau_p = 2.5$ in the presence of random noise. Initial and final states of evolution are shown below in comparison with corresponding evolution without random noise shown in Fig. 7. The evolutions with noise are depicted by the gray lines, whereas the evolutions without noise are depicted by the dashed black lines.

obvious from Fig. 8, the soliton envelope is stable against random perturbations. Moreover, the velocity of the soliton remains the same as in case of the absence of perturbations. Referring to Fig. 8, we have initial and final envelopes of the soliton after its propagation through the sample with noise and without it up to $\tau = 200$.

These figures suggest that the soliton remains stable against random noise arising in the sample. In other words, the profile of the soliton retains its shape on the background of noise, and it propagates at the same velocity, as in the absence of noise. The same situation is observed for the soliton corresponding to the lower branch of inverse square velocity (55) (see Fig. 9).

D. Inelastic collision of solitons

Of fundamental interest are the collisions of solitons in the framework of model (26)–(29). Figure 10 demonstrates the collision of the solitons of the similar and different branches at different evolution times. The initial state is depicted by the dot-dashed line, the moment of the collision is depicted by the gray solid line, and final state is depicted by the black solid line. It is evident from Fig. 10 that the solitons belonging to the upper branch collide "more" inelastically as compared to the solitons belonging to the lower branch. The reason for this is obvious: a more intensive interaction of the upper-branch solitons with two-level atoms. The collisions of solitons assigned to different branches diverge considerably. Figure 10(c) illustrates the collision between the lower branch soliton moving from the left and the upper branch soliton moving from the right. As seen from the evolution profiles, the lower branch soliton is subjected to a more significant distortion upon scattering on the upper branch soliton (see Fig. 10).

Here we should also point out that the collision of solitons, depending on the parameters, can be more complex. Inelasticity may be strong and can lead to a significant distortion of one or both solitons.

E. Formation of bistable solitons as a boundary value problem

Up to now, considering the interaction and propagation of bistable solitons, we have assumed that the solitons are formed in advance and thus we have assumed that the initial field distribution in the medium corresponds exactly to the analytical expressions. On the other hand, an important issue is the formation of solitons from pulses at the boundary of the sample. In other words, we must show that by changing the boundary conditions, it is possible to achieve the formation of solitons corresponding to both the upper and lower branches. Below, for simplicity, we consider the formation of solitons in the absence of the local field (dipole-dipole interactions). We only note here that the formation of solitons influenced by the local field does not result in additional special features. Additionally, the influence of the local field tells only on the nonlinear phase modulation of pulses and changes in initial conditions.

To formulate the boundary conditions, let us choose a pulse that is phase modulated and shaped to be of a simple form

$$E(\zeta = 0, \tau) = A_0 \frac{\exp(-i\lambda\tau)}{\cosh[(\tau - \tau_0)/\beta]}. \quad (59)$$

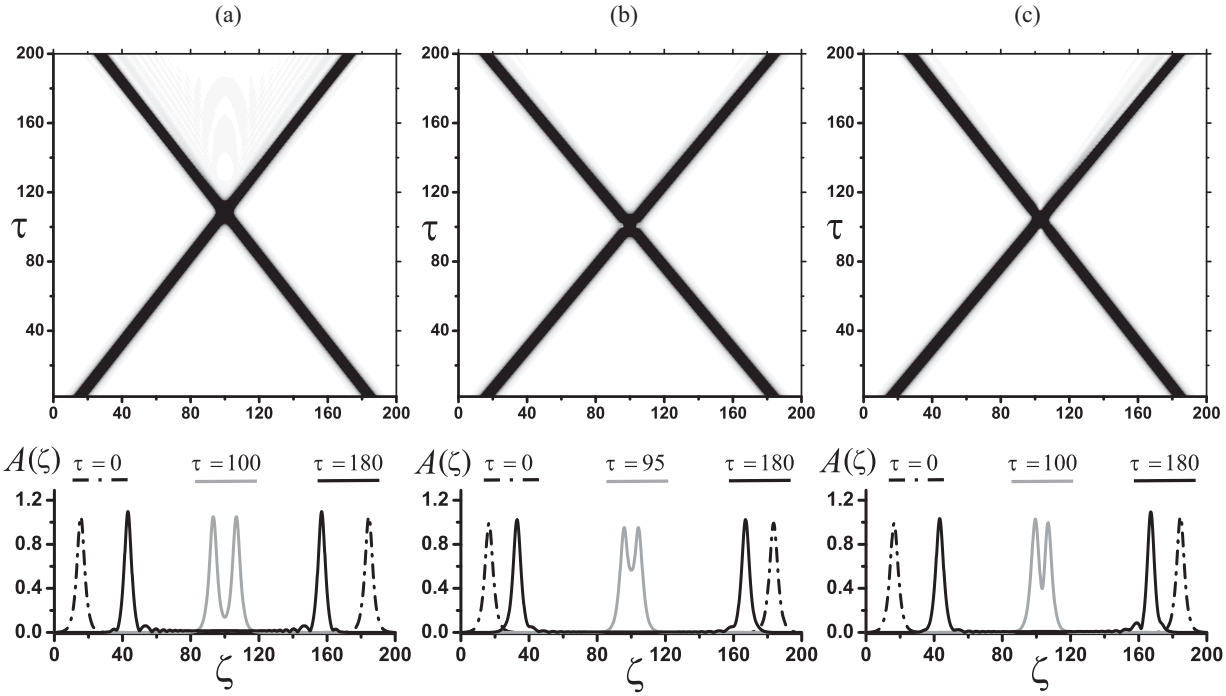

FIG. 10. Collision of solitons of Figs. 1 and 2 at $\tau_p = 2.5$ and envelopes of the solitons collusion at different times. (a) is the collision of the upper branch solitons, (b) is the collision of the lower branch solitons, and (c) is the collision of the lower branch soliton (moving from right to left) and the upper branch soliton (moving from left to right). Initial states are specified by the dot-dashed line, the moment of the collusion is specified by the gray solid line, and the final state is specified by the black solid line.

It is intended that the soliton formation occurs in compliance with the curve of Fig. 3. The envelopes of the field and population inversion are shown in Fig. 4 (the pulse duration $\tau_p = 1.5$).

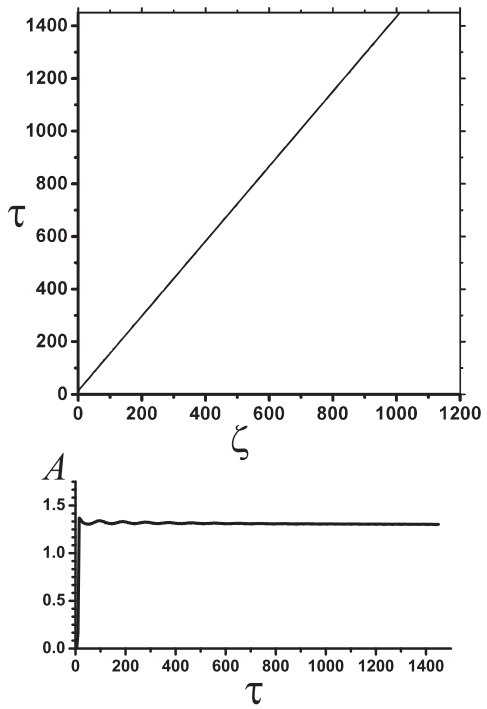

FIG. 11. Evolution of A at the formation of the upper branch soliton of Figs. 3 and 4 (at the top) and evolution of the maximum of A at different instants of time (at the bottom).

The process of formation of the soliton corresponding to the upper branch occurs in the manner indicated in Fig. 11 (at $A_0 = 1.66$, $\beta = 1.4$, $\tau_0 = 10\beta$, and $\lambda = 0.24$). Figure 11 illustrates time-dependent evolution of the maxima of the soliton envelope A at different instants. The soliton takes on its form and phase and becomes unchangeable upon completion of some transient process within a time about 200, which can be estimated from the tendency of the amplitude to a steady value. Comparison of the pulse envelope and the population inversion at a time of 1250 (at the end of its formation) is shown in Fig. 12. The envelopes are seen to be nearly the same.

The formation of the soliton corresponding to the lower branch is depicted in Fig. 13 (at $A_0 = 1.0, \beta = 2.55, \tau_0 = 10\beta$, and $\lambda = -3.7$). It differs significantly from the formation of the upper branch soliton. Figure 13 also shows the evolution of the maxima (amplitudes) of the soliton envelope A versus time. It turns out that the formation time of the soliton increases significantly in comparison with the time of upper branch soliton formation. The soliton maxima varied in the vicinity of the value predicted by the analytical expression, and tend to it with soliton propagation along the sample. Comparison of the pulse envelopes at the final stage of evolution is shown in Fig. 14 ($\tau = 1450$). One can see here that the envelopes slightly differ.

It is obvious that distinctions in the formation of soliton pulses are directly related to the efficiency of their interaction with resonant atoms. Judging from Figs. 2 and 4, the upper branch soliton interacts with two-level atoms more effectively.

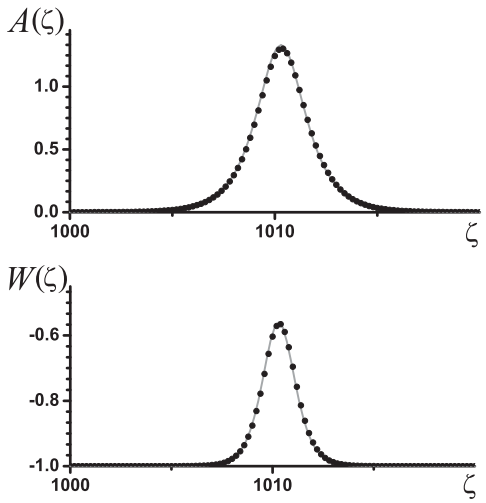

FIG. 12. Field A and the population inversion envelopes W at the final stage ($\tau = 1450$) of evolution shown in Fig. 11 (depicted by dots) as compared to the corresponding stationary soliton envelopes shown in Fig. 4 (sketched by the solid gray line).

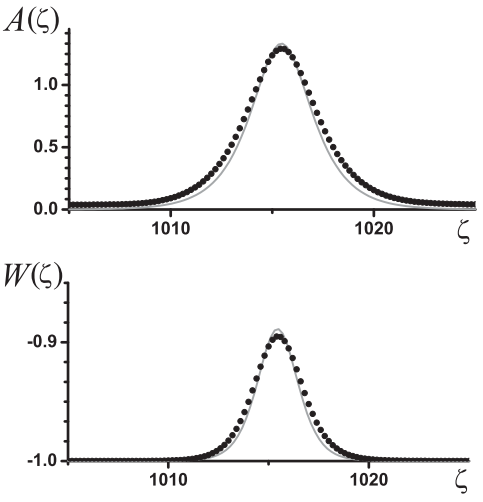

FIG. 14. Envelopes of the field A and the population inversion W at the final stage ($\tau = 1250$) of evolution shown in Fig. 13 (depicted by dots) as compared to the corresponding stationary soliton envelopes shown in Fig. 4 (sketched by the solid gray line).

This leads to its rapid formation and a slower propagation of it along the sample.

V. EXPERIMENTAL REALIZATION

As a matter of fact, some credible materials have already been proposed. For the experimental realization of SIT solitons, in Refs. [7,8,11] it was suggested to use quantum wells embedded in a semiconductor structure with the periodically alternating linear index of refraction Refs. [7,8,11]. The

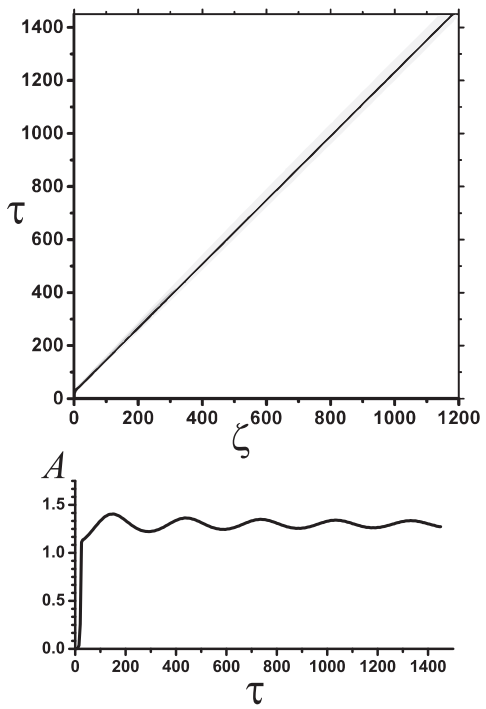

FIG. 13. Evolution of A at the formation of the lower branch soliton of Figs. 3 and 4 (at the top) and evolution of the maximum of A at different instants of time (at the bottom).

estimations presented in Refs. [7,8,11] provide the average refractive index of the periodic structure $n_0 \approx 3.6$ at the wavelength (in the medium) $\lambda \approx 232$ nm ($\omega_c \approx 2.26 \times 10^{15}$ s^{-1}) with the modulation depth $a_1 \approx 0.3$. The excitons in quantum wells at bulk densities about $\sigma_0 \approx 10^{15}$–10^{16} cm^{-3} [or surface density of $\sigma(z_j) \approx 10^{10}$–$10^{11}$ cm^{-2}) may be identified with two-level resonant centers. The estimation of the characteristic absorption time yields $\tau_0 \approx 10^{-13}$–10^{-12} s (at an electron-hole displacement of about 1–10 nm). In this case η can vary from 0 to 100 and the unit of dimensionless detuning δ is 10^{-3}–10^{-2} fraction of $\omega_c = 2\pi/\lambda$. The main disadvantage of such a suggestion is the fact that the dephasing time for excitons is rather small: $T_2 \approx 10^{-13}$ s. This means that the duration of the pulses should be $\tau_p \lesssim 10^{-14}$ s, which is close to the validity of slowly varying envelope approximation. To prolong the dephasing T_2, the temperature of the sample should be decreased up to cryogenic temperatures.

In our opinion, the most attractive approach for the realization of resonant absorption in Bragg reflectors is the use of thin layers of quantum dots. Large dipole moments of quantum dots result in a noticeable influence of the local field even at relatively low concentrations of the resonant centers because the Lorentz frequency ω_L is proportional to the square of the dipole moment. Allowance for the local field in the interaction of radiation with an ensemble of quantum dots may be made by analogy with conventional materials [26] with the result that the modified optical Bloch equations are adequate for this case, too [27,28].

As before, the layers of quantum dots should be located in the maxima of the refractive index of semiconductor media and there must be the refractive index modulation. Usage of such semiconductor media creates the conditions for the realization of various regimes of lasing due to a relative ease of modifying the properties of resonant centers.

To our knowledge, the authors of Ref. [29] were the first to observe the self-induced transparency in InGaAs quantum-dot-containing waveguides. Below we estimate the possibility of creation of periodic resonant media using layers of quantum

dot parameters where the self-induced transparency has been observed [29]. The experimental observation of self-induced transparency was preceded by the observation of Rabi oscillations at cryogenic temperatures [30], measurement of the dephasing time in a wide range of temperatures [31], and the theoretical justifications of the possibility of observation of phenomena [32].

The main advantage of using InGaAs is a relatively long dephasing time, which is close to the radiative lifetime limit at cryogenic temperatures and relatively long for higher temperatures (for example, at the temperature $T \approx 100$ K the dephasing time is $T_2 \approx 10$ ps [31]). Some other parameters are close to those estimated in [7,8,11] for exitons in quantum wells. Namely, bulk densities are about 10^{15}–10^{16} cm^{-3} (with a surface density of 10^{10}–10^{11} cm^{-2}), an average refractive index of the periodic structure n_0 is about 3.3 at the wavelength (in the medium) $\lambda \approx 324$ nm ($\omega_c \approx 5.3 \times 10^{14}$ s^{-1}), and a dipole matrix element μ is about 10^{-17}–10^{-16} esu cm ($\mu \approx 10$–100 D) [29–32]. The characteristic absorption time for quantum dot is estimated as $\tau_0 \approx 10^{-13}$–10^{-12} s. Large values of the dipole matrix elements, in spite of a relatively low concentration of quantum dots, provide a noticeable value of the Lorentz frequency w_L. For the above-mentioned parameters, the dimensionless local-field parameter can be estimated to be $\varepsilon \approx 10^{-2}$–$10^{-1}$. For comparison, the transition dipole moment of the erbium atom is a few thousandths Debye, which makes the influence of local field negligible up to the bulk concentration of resonant centers $\sigma_0 \approx 10^{20}$ cm^{-3}.

VI. CONCLUSION

In summary, we have demonstrated the bistability of SIT solitons in periodic resonant media (resonant photonic crystals) where their propagation is influenced not only by the resonant nonlinearity resonance, but by the Bragg reflection and local field as well. We succeeded in finding an analytical solution to the relevant set Maxwell-Bloch equations. This made it possible to reveal special features of the formation of bistable solitons. At that the very definition of the bistability is somewhat modified. In contrast to the case of cubic-quintic media [23,24] it is not necessary, in general, for the envelopes to differ in amplitude (peak); they may differ in spatial extension along the propagation coordinate, being equal in amplitude. Such type of bistability can exist in the absence of the local field and depends only on there being Bragg reflection. The local field fails by itself (without the Bragg reflection) to result in the bistability. However, while acting jointly, the local field is capable of enhancing the exhibition of the bistability to result in a difference between envelopes in amplitude, too.

These findings are rather unexpected and count in favor of the Bragg reflection as a basic mechanism of the bistability. It seems to us that our treatment of the bistability of the SIT solitons in periodic media is meaningful conceptually: indeed, we are dealing here with two allowed velocities (and thus with two allowed envelopes). This viewpoint correlates well with the nature of self-induced transparency, according to which there must be a fundamental relationship between the velocity and soliton duration. It is remarkable that this relationship becomes two-valued to account for the bistability.

The bistability and stability of the solitons revealed, their interactions and the boundary value problem have been reinforced with numerical simulations using the fourth-order accurate integration algorithm. It has also been shown that the bistable solitons are stable against stochastic perturbations and the collision of solitons is, in the general case, inelastic. The theory developed and computer experiment data are in good agreement.

The experimental realization of SIT periodical media seems to be archived by various ways and means. It is our opinion that the most promising approach is to take advantage of semiconductor structures which allow producing a deep modulation of the refractive index and using quantum dots as resonant centers. Their properties can be changed in a wide range and allow the observation of soliton formation to be brought about at relatively high temperatures. The above theory is best suited to such SIT experiment, and it is hoped that this can stimulate further combined investigations into the soliton propagation in resonant Bragg gratings.

ACKNOWLEDGMENTS

The authors are grateful to Professor B. I. Mantsysov for the discussion of the results as well as to an anonymous referee for constructive criticism and recommendations. The work was supported by Belarusian Republican Foundation for Fundamental Research (Grant BRFFI No. F09-017).

[1] B. Mantsyzov and R. Kuz'min, Sov. Phys. JETP **64**, 37 (1986).
[2] B. I. Mantsyzov, Phys. Rev. A **51**, 4939 (1995).
[3] T. Lakoba and B. Mantsyzov, Bull. Russ. Acad. Sci. Phys. **56**, 1205 (1992).
[4] B. Mantsyzov, JETP Lett. **82**, 253 (2005).
[5] B. Mantsyzov and R. SilNikov, JETP Lett. **74**, 456 (2001).
[6] B. I. Mantsyzov, *Coherent and Nonlinear Optics of Photonic Crystals/Kogerentnaya i nelineynaya optika fotonnykh kristallov* (in Russian) (Fizmatlit, Moscow, 2009).
[7] G. Kurizki, A. E. Kozhekin, T. Opatrny, and B. A. Malomed, in *Progress in Optics*, edited by E. Wolf, Vol. 42 (Elsevier, Amsterdam, 2001), pp. 93–146.
[8] T. Opatrný, B. A. Malomed, and G. Kurizki, Phys. Rev. E **60**, 6137 (1999).
[9] A. Kozhekin and G. Kurizki, Phys. Rev. Lett. **74**, 5020 (1995).
[10] A. E. Kozhekin, G. Kurizki, and B. Malomed, Phys. Rev. Lett. **81**, 3647 (1998).
[11] J. Cheng and J. Zhou, Phys. Rev. E **66**, 036606 (2002).
[12] C. M. Bowden and J. P. Dowling, Phys. Rev. A **47**, 1247 (1993).
[13] J. J. Maki, M. S. Malcuit, J. E. Sipe, and R. W. Boyd, Phys. Rev. Lett. **67**, 972 (1991).
[14] M. E. Crenshaw, M. Scalora, and C. M. Bowden, Phys. Rev. Lett. **68**, 911 (1992).

[15] J. P. Dowling and C. M. Bowden, Phys. Rev. Lett. **70**, 1421 (1993).
[16] N. Wang and H. Rabitz, Phys. Rev. A **51**, 5029 (1995).
[17] M. E. Crenshaw and C. M. Bowden, Phys. Rev. Lett. **85**, 1851 (2000).
[18] J. T. Manassah and I. Gladkova, Opt. Commun. **196**, 221 (2001).
[19] A. A. Afanas'ev, R. A. Vlasov, O. K. Khasanov, T. V. Smirnova, and O. M. Fedotova, J. Opt. Soc. Am. B **19**, 911 (2002).
[20] A. Afanas'ev, R. Vlasov, and A. Cherstvyi, J. Exp. Theor. Phys. **90**, 428 (2000).
[21] K. Xia, S. Gong, C. Liu, X. Song, and Y. Niu, Opt. Express **13**, 5913 (2005).
[22] D. V. Novitsky, Phys. Rev. A **79**, 023828 (2009).
[23] S. Gatz and J. Herrmann, J. Opt. Soc. Am. B **8**, 2296 (1991).
[24] J. Herrmann, Opt. Commun. **87**, 161 (1992).
[25] C. M. de Sterke, K. R. Jackson, and B. D. Robert, J. Opt. Soc. Am. B **8**, 403 (1991).
[26] S. Maksimenko, G. Slepyan, A. Hoffmann, and D. Bimberg, Phys. Status Solidi A **190**, 555 (2002).
[27] G. Y. Slepyan, A. Magyarov, S. A. Maksimenko, A. Hoffmann, and D. Bimberg, Phys. Rev. B **70**, 045320 (2004).
[28] E. Paspalakis, A. Kalini, and A. F. Terzis, Phys. Rev. B **73**, 073305 (2006).
[29] S. Schneider, P. Borri, W. Langbein, U. Woggon, J. Förstner, A. Knorr, R. L. Sellin, D. Ouyang, and D. Bimberg, Appl. Phys. Lett. **83**, 3668 (2003).
[30] P. Borri, W. Langbein, S. Schneider, U. Woggon, R. L. Sellin, D. Ouyang, and D. Bimberg, Phys. Rev. B **66**, 081306 (2002).
[31] P. Borri, W. Langbein, S. Schneider, U. Woggon, R. L. Sellin, D. Ouyang, and D. Bimberg, Phys. Rev. Lett. **87**, 157401 (2001).
[32] G. Panzarini, U. Hohenester, and E. Molinari, Phys. Rev. B **65**, 165322 (2002).